




Article

Facile and Green Synthesis of Graphene-Based Conductive Adhesives via Liquid Exfoliation Process

Jhao-Yi Wu ¹, Yi-Chin Lai ², Chien-Liang Chang ³, Wu-Ching Hung ³, Hsiao-Min Wu ³, Ying-Chih Liao ^{2,*} , Chia-Hung Huang ⁴ and Wei-Ren Liu ^{1,*}

¹ Department of Chemical Engineering, Chung Yuan Christian University, R&D Center for Membrane Technology, 32023, No. 200, Chun Pei Rd., Chung Li District, Taoyuan 32023, Taiwan; james19931201@gmail.com

² Department of Chemical Engineering, National Taiwan University, No. 1, Sec. 4, Roosevelt Rd., Taipei 10617, Taiwan; yijin10221339@gmail.com

³ National Chung Shan Institute of Science & Technology, Neighborhood, Sec. Jia'an, Zhongzheng Rd., Longtan Dist., Taoyuan 32546, Taiwan; rodin2005@yahoo.com.tw (C.-L.C.); 5000blackblue@gmail.com (W.-C.H.); prettysandy119@gmail.com (H.-M.W.)

⁴ Metal Industries Research and Development Centre, Kaohsiung 81160, Taiwan; chiahung@mail.mirdc.org.tw

* Correspondence: liaoy@ntu.edu.tw (Y.-C.L.); WRLiu1203@gmail.com (W.-R.L.); Tel.: +886-3-265-4140 (W.-R.L.); Fax: +886-3-265-4199 (W.-R.L.)

Received: 11 December 2018; Accepted: 23 December 2018; Published: 28 December 2018



Abstract: In this study, we report a facile and green process to synthesize high-quality and few-layer graphene (FLG) derived from graphite via a liquid exfoliation process. The corresponding characterizations of FLG, such as scanning electron microscopy (SEM), transmission electron microscope (TEM), atomic force microscopy (AFM) and Raman spectroscopy, were carried out. The results of SEM show that the lateral size of as-synthesized FLG is 1–5 μm . The results of TEM and AFM indicate more than 80% of graphene layers is <10 layers. The most surprising thing is that D/G ratio of graphite and FLG are 0.15 and 0.19, respectively. The result of the similar D/G ratio demonstrates that little structural defects were created via the liquid exfoliation process. Electronic conductivity tests and resistance of composite film, in terms of different contents of graphite/polyvinylidene difluoride (PVDF) and FLG/PVDF, were carried out. Dramatically, the FLG/PVDF composite demonstrates superior performance compared to the graphite/PVDF composite at the same ratio. In addition, the post-sintering process plays an important role in improving electronic conductivity by 85%. The composition-optimized FLG/PVDF thin film exhibits $81.9 \text{ S}\cdot\text{cm}^{-1}$. These results indicate that the developed FLG/PVDF composite adhesives could be a potential candidate for conductive adhesive applications.

Keywords: graphene; liquid exfoliation; polyvinylidene fluoride; conductive adhesives; flexible

1. Introduction

Electronics or microelectronics industries have transitioned into making electronics lighter, smaller, thinner and more highly efficient [1,2]. Aside from this, they must employ techniques and materials that are environmentally friendly. As a result, they opt to replace lead-based solders for microelectronics packaging with electrically conductive adhesives (ECAs). A great deal of research has been carried out on the fabrication of polymer composites reinforced by metallic fillers ranging from metallic particles to carbon materials. These polymer composites have been used to develop new types of ECAs to reduce the cost to provide finer pitch capability [3]. Gold, silver [4–7], copper [8], palladium and nickel have been widely used as fillers for commercial ECAs due to their stability and excellent electrical conductivity [7,9]. However, a high concentration of filler is required to form a good electrical

conductivity [5], which is the main reason for the high cost of ECAs. How to reduce the loading of metal fillers into the ECAs has become an important issue.

Many researches use carbon nanotubes (CNTs) [10–12] as fillers to improve the electrical properties of ECAs due to their high conductivity, flexibility, and large aspect ratios, and report the establishment of a percolated network at low filler content. However, the usage of CNTs has been limited by the challenges in processing, high cost and dispersion [13]. As a two-dimensional material, graphene has attracted wide attention due to its stable structure and excellent performance. These materials have drawn an intensive attention towards a variety of research fields to utilize their exceptional thermal, mechanical, optical and electrical properties [14–16]. Theoretical and experimental studies of graphene show they may possess high thermal conductivity ($5000 \text{ W}\cdot\text{m}^{-1}\cdot\text{K}^{-1}$), high Young's modulus ($\sim 1 \text{ TPa}$), large surface area ($\sim 2600 \text{ m}^2\cdot\text{g}^{-1}$) [17,18] and great electrical conductivity ($6000 \text{ S}\cdot\text{cm}^{-1}$) [19]. Possessing the extremely high aspect ratio among all the nanostructured materials, graphene is a promising nanomaterial able to establish a percolated network at very low concentrations.

Xie et al. predicted that in comparison with nanotubes, graphene could provide higher conductivity when used as fillers for conductive adhesives. This is due to its large specific area [20–22]. Electrical conductivities of auxiliary forms of graphene have also been reported and studied as conductive fillers or reinforcements for polymers. The polypropylene/graphene oxide (PP/GO) nanocomposite prepared by Huang and colleagues through Ziegler-Natta polymerization provides a high conductivity of $0.3 \text{ S}\cdot\text{m}^{-1}$ at a 4.9 wt.% loading of GO [23,24]. The chemically reduced graphene oxide/polystyrene (CRGO/PS) composite prepared by Stankovich [25] delivers $0.1 \text{ S}\cdot\text{m}^{-1}$. Qi et al. [26] compared the electrical conductivity of MWCNT/PS and G/PS nanocomposites and found that at 0.69 wt.%, G/PS has a conductivity of $3.49 \text{ S}\cdot\text{m}^{-1}$ while MWCNT/PS at the same content only has a conductivity of $3 \times 10^{-5} \text{ S}\cdot\text{m}^{-1}$. Ansari et al. studied and compared the properties of functionalized graphene sheet/PVDF (FGS/PVDF) and exfoliated graphite/PVDF (EG/PVDF), which were prepared via a solution process with subsequent compression to fabricate conductive nanocomposites. According to their results, FGS remained well dispersed in PVDF and showed wrinkled topography with relatively thin graphene sheets that were bonded well in the matrix [27].

In order to obtain graphene, various methods, such as exfoliation and cleavage, liquid-phase exfoliation [28,29], growth on SiC [30,31], chemical vapor deposition [32,33], molecular beam epitaxy, chemical synthesis [34–37], and chemical routes, have been widely studied. Mass production of single-layer graphene or few-layer graphene is being hindered by the expensive cost and environmental threat of its conventional synthesis. From the environmentally friendly viewpoint, there are many researches that have studied the synthesis of graphene by a simple ultrasonication or jet cavitation method to obtain few-layer graphene [38]. In this paper, a low-temperature, high-pressure continuous flow cell disrupter was used as a delamination device to synthesize few-layer graphene. With this method, simple, scalable, low-cost graphene was swiftly produced without the incorporation of any toxic chemicals. The graphene obtained by this method was combined with polymer to make ECAs.

2. Experimental

2.1. Synthesis of FLG

Natural flake graphite ($\text{Ø}_{\text{ave}} = 500 \text{ }\mu\text{m}$) was used as a feed material for the delamination process while *N*-Methyl-2-pyrrolidone (NMP) and polyvinylidene fluoride (PVDF) purchased from UBIQ Technology Co. Ltd., Taiwan were used as a dispersing agent and a binder, respectively. The synthesis of FLG was described as follow: a 1 kg solution consisting of 10 wt.% natural graphite dispersed in de-ionized water ($\text{DI H}_2\text{O}$) was fed into a low-temperature, ultra-high-pressure continuous flow cell disrupter (LTHPD, JNBIO, JN 10C, Guangzhou, China). Prior to feeding the solution into the tank of the LTHPD, the solution was vigorously stirred to ensure uniform dispersion. The graphite solution was pumped into a nozzle with a high pressure and a high flow rate. Under the high-pressure, strong-impact and repeated cyclic stress, layers of graphite were exfoliated, obtaining few-layer

graphene (FLG). LTHPD did not only delaminate the graphite flakes into FLG, but also ensures homogeneous dispersion in the solution. The operating condition was maintained at 1800 bar and 14–16 °C. The obtained product was dried in a vacuum oven at 30 °C overnight.

2.2. Conductive Adhesive Slurry Preparations

Different slurry compositions were prepared with various FLG:PVDF ratios, such as 1:99, 5:95, 8:92, 10:90, 30:70, 90:90, and 50:50 by dispersing PVDF with a designated amount into NMP. After ensuring the homogeneity of PVDF in NMP, FLG was added into the solution and stirred for 2 h. The slurry was coated onto glass slides and dried at 80 °C for 1 h. The graphite:PVDF slurry of the same compositions was also prepared for comparison.

2.3. Characterizations

The height profile of as-synthesized few-layer graphene was measured by using atomic force microscopy (AFM, Bruker Dimension Icon). The samples for AFM were prepared by dropping the dispersion directly onto a freshly cleaved mica wafer. Raman spectra were carried out by a micro Raman spectroscopy system with a laser frequency of 532 nm as the excitation source. The morphologies of the samples were analyzed using scanning electron microscopy (SEM) by Hitachi S-4100 (Hitachi, Tokyo, Japan) and high-resolution transmission electron microscopy (HRTEM) JEOL-JEM2000FXII (JEOL, Tokyo, Japan). The electrical conductivities of the graphene adhesives were measured using a resistivity meter (KeithLink TG2, KeithLink, Taipei, Taiwan) with a four-point probe.

3. Results and Discussion

3.1. Characterizations of FLG

Figure 1a,b show images of graphite and FLG with lateral sizes of 5–10 μm and 1–5 μm , respectively. After treatment by LTHPD, the graphite size was decreased and delaminated to be FLG. This shows that the thick sheets of graphite can be effectively exfoliated into thinner sheets. Figure 1c displays the HRTEM image of the FLG. This image of FLG is transparent and folded, which coincides well with the typical feature of the reported FLG. In order to observe the effect of the LTHPD, AFM characterization was carried out for its convenience in measuring flake thickness. The FLG was deposited on the silica wafer and dried in room temperature. More than 30 flakes were measured to determine the distribution. Figure 1d,e show the AFM image and the thickness distribution of FLG. They are believed to be monolayers according to the fact that FLG are often measured to be 0.4–1 nm by AFM due to some external factors such as the AFM equipment and substrates [39,40]. This shows that the range of FLG thickness is 1–4.5 nm, which is less than 10 layers. The delamination process used to obtain FLG was expected to cause defects, and thus, Raman analysis of graphite and FLG was determined and is depicted in Figure 1f. The result of similar D/G ratio demonstrates that little structural defects were created by the liquid exfoliation process. Additionally, the intensity ratio of D/G for the FLG is 0.19, which is much lower than that of the GO and chemically reduced graphene [41,42].

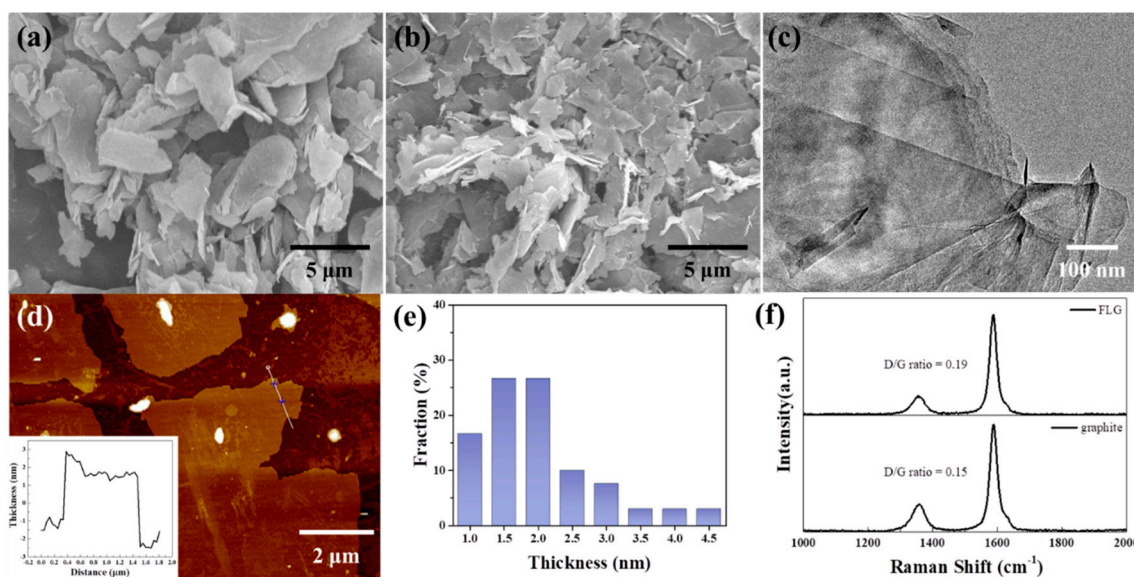


Figure 1. SEM images of (a) graphene and (b) FLG; (c) TEM image of FLG; (d) AFM image of FLG, insert: height profiles of FLG; (e) thickness distribution of FLG measured by AFM on 35 samples; (f) Raman spectra of graphite and FLG.

3.2. Characterizations of Conductive Adhesives

To formulate conductive adhesives, the conductive fillers, graphite and FLG were mixed with PVDF. After mixing, the composites inks were cast into a 2×2 mm well to create solid thin films (Figure 2). The dried thin films at various filler/PVDF ratios exhibit color variations. The FLG/PVDF composite also exhibits great conductivity compared to its graphite counterpart. As shown in Figure 3, at the same filler/PVDF ratio, the conductivity of the FLG/PVDF composite is always higher than that of the graphite/PVDF composite, which is possibly due to the higher aspect ratio of FLG. The lateral size of FLG is $\sim 8 \mu\text{m}$ and the average thickness of FLG is ~ 4 nm. Thus, the aspect ratio of as-synthesized FLG is as high as ~ 2000 . The higher aspect ratio provided a better percolation network for electron transfer, and thus resulted in the conductivity enhancement.

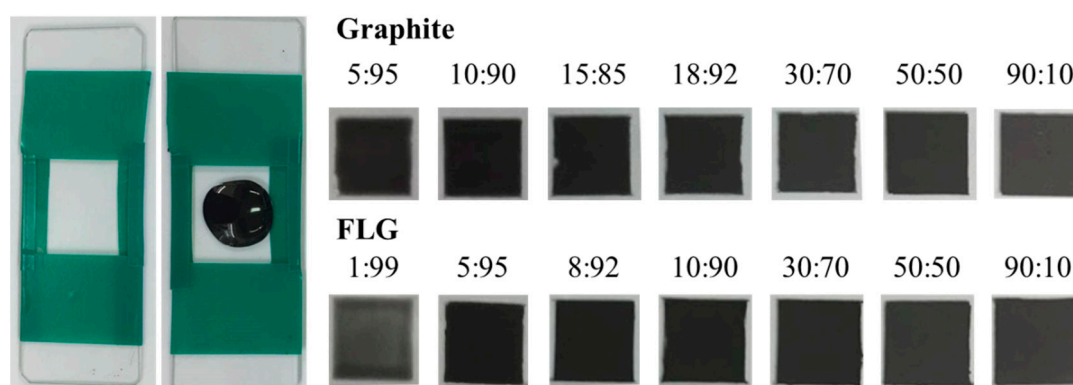


Figure 2. Photo images of graphite/PVDF and FLG/PVDF composites.

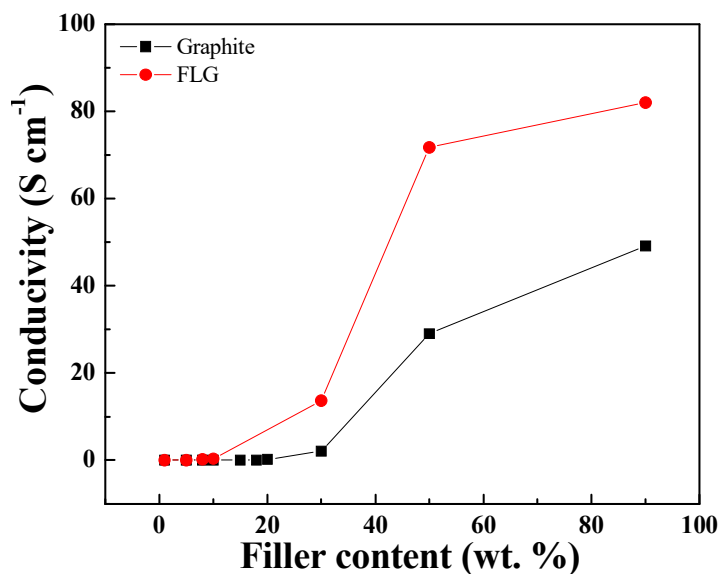


Figure 3. Electronic conductivity of graphite/PVDF and FLG/PVDF composite films measured by a four-point probe.

The conductivity of the FLG/PVDF thin film can be greatly enhanced after sintering. As shown in Figure 4, when the temperature increases, the resistance decreases. This reduction of resistivity comes from relaxation of the polymer chains at higher temperatures and thus leads to a decrease in the mean distance between graphene [43–45]. The shortened distance between graphene layers helps the electron transfer and thus increases the conductivity [46]. However, as the temperature reaches the glass transition temperature of PVDF from ~400 to 425 °C, the relaxation process facilitates the re-arrangement of the dispersed graphene [45] and thus the resistance plateau occurs at ~400 °C.

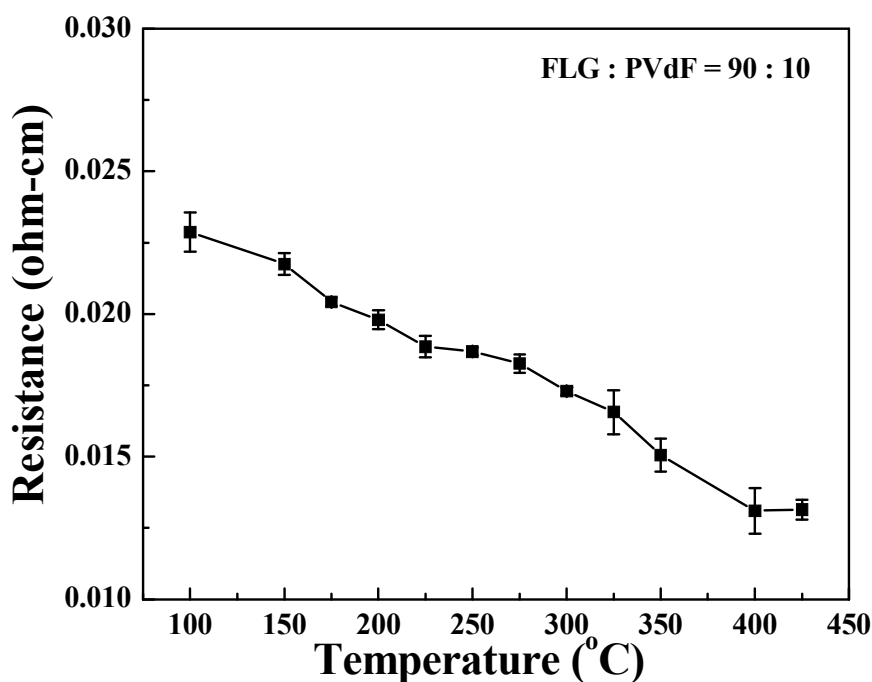


Figure 4. Variation in sheet resistance of FLG/PVDF composite films with temperature. The FLG/PVDF thin film is coated on glass with a thickness of 0.02 mm and is placed on a hot plate for 30 min.

The FLG/PVDF composite also exhibits great flexibility and mechanical strength after being coated on flexible plastic sheets. The electrical resistance of the FLG/PVDF thin film on the PET film

under the bending test (inset picture in Figure 5a) shows a fairly small variation after thousands of bending cycles. The small increase of ~5% in resistance is possibly attributed to the crack of film under bending [47]. This great mechanical strength makes the FLG/PVDF a great conductive adhesive for flexible electronic applications. For demonstration, two pieces of printed FLG/PVDF thin films on the PET film were connected to an LED, and the printed conductive tracks were twisted or bent with different degrees of curvature (Figure 5b,d). As shown in Figure 5c, the PET film with slight curvature could remain bright. The bulb shone constantly after bending the film into a spiral shape, as shown in Figure 5d, indicating the great bending property of the graphene/PVDF composites on the PET film.

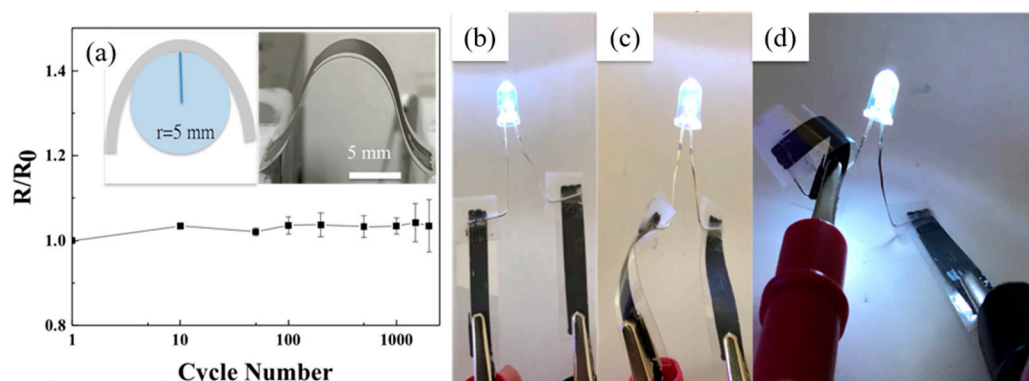


Figure 5. (a) The resistance increase ratio (R/R_0) of graphene/PVDF thin film on the PET film under the bending performance test with a radius of curvature of 5 mm. After connecting the graphene/polymer composite to an LED, the light remained bright at various degrees of bending: (b) flat, (c) bending, and (d) spiral shape.

4. Discussion

In this study, a facile liquid exfoliation process was developed to synthesize FLG. Electron microscopic examination shows the as-synthesized FLG has a lateral size of 1–5 μm . AFM indicates more than 80% of FLG has less than 10 layers. Raman spectroscopy also shows a great D/G ratio of 0.19, which is close to that of graphite (0.15), indicating that little structural defects were created via the liquid exfoliation process. After being mixed with PVDF, the composite FLG/PVDF thin film exhibits superior electronic conductivity compared to the graphite/PVDF composite with the same ratio. Moreover, the post-sintering process can further improve electronic conductivity by 85%. The composition-optimized FLG/PVDF composite exhibits $81.9 \text{ S}\cdot\text{cm}^{-1}$. The printed FLG/PVDF thin film patterns also show great flexibility and mechanical strength under bending conditions. The electrical conductivity remains nearly the same after thousands of bending cycles. These results indicate that the formulated FLG/PVDF composite adhesives have a great potential in conductive adhesive applications.

Author Contributions: J.-Y.W. synthesize few layer graphene. Y.-C.L. assemble different ratio of graphene/PVDF as composite film. J.-Y.W. and Y.-C.L. write the manuscript. C.-L.C., W.-C.H., C.-H.H. and H.-M.W. help to characterize the properties of graphene/PVDF film. Y.-C.L. and W.-R.L. are supervisors to guide experiment and manuscript refine.

Funding: This research is supported by the National Science Council of Taiwan under contract numbers: 102-2221-E-033-050- MY2, 102-3011-P-033-003, and MOST 106-2218-E-002-038.

Conflicts of Interest: The authors declare no conflicts of interest.

References

1. Périchaud, M.-G.; Delétage, J.-Y.; Frémont, H.; Danto, Y.; Faure, C. Reliability evaluation of adhesive bonded SMT components in industrial applications. *Microelectron. Reliab.* **2000**, *40*, 1227–1234. [[CrossRef](#)]

2. Daniel Lu, D.; Grace Li, Y.; Wong, C. Recent advances in nano-conductive adhesives. *J. Adhes. Sci. Technol.* **2008**, *22*, 815–834. [[CrossRef](#)]
3. Li, Y.; Moon, K.-S.; Wong, C. Electronics without lead. *Science* **2005**, *308*, 1419–1420. [[CrossRef](#)] [[PubMed](#)]
4. Ye, L.; Lai, Z.; Liu, J.; Tholen, A. Effect of Ag particle size on electrical conductivity of isotropically conductive adhesives. *IEEE Trans. Electron. Packag. Manuf.* **1999**, *22*, 299–302.
5. Kotthaus, S.; Gunther, B.H.; Hang, R.; Schafer, H. Study of isotropically conductive bondings filled with aggregates of nano-sited Ag-particles. *IEEE Trans. Electron. Packag. Manuf.* **1997**, *20*, 15–20. [[CrossRef](#)]
6. Lee, H.-H.; Chou, K.-S.; Shih, Z.-W. Effect of nano-sized silver particles on the resistivity of polymeric conductive adhesives. *Int. J. Adhes. Adhes.* **2005**, *25*, 437–441. [[CrossRef](#)]
7. Wu, H.; Liu, J.; Wu, X.; Ge, M.; Wang, Y.; Zhang, G.; Jiang, J. High conductivity of isotropic conductive adhesives filled with silver nanowires. *Int. J. Adhes. Adhes.* **2006**, *26*, 617–621. [[CrossRef](#)]
8. Zhao, H.; Liang, T.; Liu, B. Synthesis and properties of copper conductive adhesives modified by SiO₂ nanoparticles. *Int. J. Adhes. Adhes.* **2007**, *27*, 429–433. [[CrossRef](#)]
9. Jia, W.; Tchoudakov, R.; Joseph, R.; Narkis, M.; Siegmann, A. The role of a third component on the conductivity behavior of ternary epoxy/Ag conductive composites. *Polym. Compos.* **2002**, *23*, 510–519. [[CrossRef](#)]
10. Chun, K.-Y.; Oh, Y.; Rho, J.; Ahn, J.-H.; Kim, Y.-J.; Choi, H.R.; Baik, S. Highly conductive, printable and stretchable composite films of carbon nanotubes and silver. *Nat. Nanotechnol.* **2010**, *5*, 853–857. [[CrossRef](#)]
11. Ji, S.Y.; Ajmal, C.M.; Kim, T.; Chang, W.S.; Baik, S. Laser patterning of highly conductive flexible circuits. *Nanotechnology* **2017**, *28*, 165301. [[CrossRef](#)]
12. Gorrasi, G.; Sarno, M.; Di Bartolomeo, A.; Sannino, D.; Ciambelli, P.; Vittoria, V. Incorporation of carbon nanotubes into polyethylene by high energy ball milling: Morphology and physical properties. *J. Polym. Sci. Part B Polym. Phys.* **2007**, *45*, 597–606. [[CrossRef](#)]
13. Kim, J.; Yim, B.-S.; Kim, J.-M.; Kim, J. The effects of functionalized graphene nanosheets on the thermal and mechanical properties of epoxy composites for anisotropic conductive adhesives (ACAs). *Microelectron. Reliab.* **2012**, *52*, 595–602. [[CrossRef](#)]
14. Giubileo, F.; Di Bartolomeo, A.; Martucciello, N.; Romeo, F.; Iemmo, L.; Romano, P.; Passacantando, M. Contact resistance and channel conductance of graphene field-effect transistors under low-energy electron irradiation. *Nanomaterials* **2016**, *6*, 206. [[CrossRef](#)]
15. Alvarado Chavarin, C.; Strobel, C.; Kitzmann, J.; Di Bartolomeo, A.; Lukosius, M.; Albert, M.; Bartha, J.W.; Wenger, C. Current Modulation of a Heterojunction Structure by an Ultra-Thin Graphene Base Electrode. *Materials* **2018**, *11*, 345. [[CrossRef](#)]
16. Luongo, G.; Di Bartolomeo, A.; Giubileo, F.; Alvarado Chavarin, C.; Wenger, C. Electronic properties of graphene/p-silicon Schottky junction. *J. Phys. D Appl. Phys.* **2018**, *51*. [[CrossRef](#)]
17. Balandin, A.A.; Ghosh, S.; Bao, W.; Calizo, I.; Teweldebrhan, D.; Miao, F.; Lau, C.N. Superior thermal conductivity of single-layer graphene. *Nano Lett.* **2008**, *8*, 902–907. [[CrossRef](#)] [[PubMed](#)]
18. Lee, C.; Wei, X.; Kysar, J.W.; Hone, J. Measurement of the elastic properties and intrinsic strength of monolayer graphene. *Science* **2008**, *321*, 385–388. [[CrossRef](#)]
19. Du, X.; Skachko, I.; Barker, A.; Andrei, E.Y. Approaching ballistic transport in suspended graphene. *Nat. Nanotechnol.* **2008**, *3*, 491–495. [[CrossRef](#)]
20. Du, J.; Cheng, H.M. The fabrication, properties, and uses of graphene/polymer composites. *Macromol. Chem. Phys.* **2012**, *213*, 1060–1077. [[CrossRef](#)]
21. Khanam, P.N.; Ponnamma, D.; Al-Madeed, M. Electrical properties of graphene polymer nanocomposites. In *Graphene-Based Polymer Nanocomposites in Electronics*; Springer: Berlin, Germany, 2015; pp. 25–47.
22. Xie, S.; Liu, Y.; Li, J. Comparison of the effective conductivity between composites reinforced by graphene nanosheets and carbon nanotubes. *Appl. Phys. Lett.* **2008**, *92*, 243121. [[CrossRef](#)]
23. Huang, Y.; Qin, Y.; Zhou, Y.; Niu, H.; Yu, Z.-Z.; Dong, J.-Y. Polypropylene/Graphene Oxide Nanocomposites Prepared by In Situ Ziegler–Natta Polymerization. *Chem. Mater.* **2010**, *22*, 4096–4102. [[CrossRef](#)]
24. Gorrasi, G.; Bugatti, V.; Milone, C.; Mastronardo, E.; Piperopoulos, E.; Iemmo, L.; Di Bartolomeo, A. Effect of temperature and morphology on the electrical properties of PET/conductive nano fillers composites. *Compos. Part B Eng.* **2018**, *135*, 149–154. [[CrossRef](#)]
25. Stankovich, S.; Dikin, D.A.; Dommett, G.H.; Kohlhaas, K.M.; Zimney, E.J.; Stach, E.A.; Piner, R.D.; Nguyen, S.T.; Ruoff, R.S. Graphene-based composite materials. *Nature* **2006**, *442*, 282–286. [[CrossRef](#)] [[PubMed](#)]

26. Qi, X.-Y.; Yan, D.; Jiang, Z.; Cao, Y.-K.; Yu, Z.-Z.; Yavari, F.; Koratkar, N. Enhanced electrical conductivity in polystyrene nanocomposites at ultra-low graphene content. *ACS Appl. Mater. Interfaces* **2011**, *3*, 3130–3133. [[CrossRef](#)] [[PubMed](#)]
27. Ansari, S.; Giannelis, E.P. Functionalized graphene sheet—Poly (vinylidene fluoride) conductive nanocomposites. *J. Polym. Sci. Part B Polym. Phys.* **2009**, *47*, 888–897. [[CrossRef](#)]
28. Hernandez, Y.; Nicolosi, V.; Lotya, M.; Blighe, F.M.; Sun, Z.; De, S.; McGovern, I.; Holland, B.; Byrne, M.; Gun'Ko, Y.K. High-yield production of graphene by liquid-phase exfoliation of graphite. *Nat. Nanotechnol.* **2008**, *3*, 563–568. [[CrossRef](#)]
29. Lotya, M.; Hernandez, Y.; King, P.J.; Smith, R.J.; Nicolosi, V.; Karlsson, L.S.; Blighe, F.M.; De, S.; Wang, Z.; McGovern, I. Liquid phase production of graphene by exfoliation of graphite in surfactant/water solutions. *J. Am. Chem. Soc.* **2009**, *131*, 3611–3620. [[CrossRef](#)]
30. Virojanadara, C.; Syväjärvi, M.; Yakimova, R.; Johansson, L.; Zakharov, A.; Balasubramanian, T. Homogeneous large-area graphene layer growth on 6 H-SiC (0001). *Phys. Rev. B* **2008**, *78*, 245403. [[CrossRef](#)]
31. Sprinkle, M.; Ruan, M.; Hu, Y.; Hankinson, J.; Rubio-Roy, M.; Zhang, B.; Wu, X.; Berger, C.; De Heer, W.A. Scalable templated growth of graphene nanoribbons on SiC. *Nat. Nanotechnol.* **2010**, *5*, 727–731. [[CrossRef](#)]
32. Reina, A.; Jia, X.; Ho, J.; Nezich, D.; Son, H.; Bulovic, V.; Dresselhaus, M.S.; Kong, J. Large area, few-layer graphene films on arbitrary substrates by chemical vapor deposition. *Nano Lett.* **2008**, *9*, 30–35. [[CrossRef](#)] [[PubMed](#)]
33. Wei, D.; Liu, Y.; Wang, Y.; Zhang, H.; Huang, L.; Yu, G. Synthesis of N-doped graphene by chemical vapor deposition and its electrical properties. *Nano Lett.* **2009**, *9*, 1752–1758. [[CrossRef](#)] [[PubMed](#)]
34. Chen, J.; Yao, B.; Li, C.; Shi, G. An improved Hummers method for eco-friendly synthesis of graphene oxide. *Carbon* **2013**, *64*, 225–229. [[CrossRef](#)]
35. Eigler, S.; Enzelberger-Heim, M.; Grimm, S.; Hofmann, P.; Kroener, W.; Geworski, A.; Dotzer, C.; Röckert, M.; Xiao, J.; Papp, C. Wet chemical synthesis of graphene. *Adv. Mater.* **2013**, *25*, 3583–3587. [[CrossRef](#)] [[PubMed](#)]
36. Zhang, Y.; Fugane, K.; Mori, T.; Niu, L.; Ye, J. Wet chemical synthesis of nitrogen-doped graphene towards oxygen reduction electrocatalysts without high-temperature pyrolysis. *J. Mater. Chem.* **2012**, *22*, 6575–6580. [[CrossRef](#)]
37. Chen, L.; Hernandez, Y.; Feng, X.; Müllen, K. From nanographene and graphene nanoribbons to graphene sheets: Chemical synthesis. *Angew. Chem. Int. Ed.* **2012**, *51*, 7640–7654. [[CrossRef](#)] [[PubMed](#)]
38. Liang, S.; Shen, Z.; Yi, M.; Liu, L.; Zhang, X.; Cai, C.; Ma, S. Effects of Processing Parameters on Massive Production of Graphene by Jet Cavitation. *J. Nanosci. Nanotechnol.* **2015**, *15*, 2686–2694. [[CrossRef](#)]
39. Nacken, T.; Damm, C.; Walter, J.; Rüger, A.; Peukert, W. Delamination of graphite in a high pressure homogenizer. *RSC Adv.* **2015**, *5*, 57328–57338. [[CrossRef](#)]
40. Novoselov, K.S.; Geim, A.K.; Morozov, S.V.; Jiang, D.; Zhang, Y.; Dubonos, S.V.; Grigorieva, I.V.; Firsov, A.A. Electric field effect in atomically thin carbon films. *Science* **2004**, *306*, 666–669. [[CrossRef](#)]
41. Stankovich, S.; Piner, R.D.; Chen, X.; Wu, N.; Nguyen, S.T.; Ruoff, R.S. Stable aqueous dispersions of graphitic nanoplatelets via the reduction of exfoliated graphite oxide in the presence of poly (sodium 4-styrenesulfonate). *J. Mater. Chem.* **2006**, *16*, 155–158. [[CrossRef](#)]
42. Stankovich, S.; Dikin, D.A.; Piner, R.D.; Kohlhaas, K.A.; Kleinhammes, A.; Jia, Y.; Wu, Y.; Nguyen, S.T.; Ruoff, R.S. Synthesis of graphene-based nanosheets via chemical reduction of exfoliated graphite oxide. *Carbon* **2007**, *45*, 1558–1565. [[CrossRef](#)]
43. Palza, H.; Garzón, C.; Arias, O. Modifying the electrical behaviour of polypropylene/carbon nanotube composites by adding a second nanoparticle and by annealing processes. *Express Polym. Lett.* **2012**, *6*, 639–646. [[CrossRef](#)]
44. Palza, H.; Kappes, M.; Hennrich, F.; Wilhelm, M. Morphological changes of carbon nanotubes in polyethylene matrices under oscillatory tests as determined by dielectrical measurements. *Compos. Sci. Technol.* **2011**, *71*, 1361–1366. [[CrossRef](#)]
45. Cipriano, B.H.; Kota, A.K.; Gershon, A.L.; Laskowski, C.J.; Kashiwagi, T.; Bruck, H.A.; Raghavan, S.R. Conductivity enhancement of carbon nanotube and nanofiber-based polymer nanocomposites by melt annealing. *Polymer* **2008**, *49*, 4846–4851. [[CrossRef](#)]

46. Garzón, C.; Palza, H. Electrical behavior of polypropylene composites melt mixed with carbon-based particles: Effect of the kind of particle and annealing process. *Compos. Sci. Technol.* **2014**, *99*, 117–123. [[CrossRef](#)]
47. Lewis, J. Material challenge for flexible organic devices. *Mater. Today* **2006**, *9*, 38–45. [[CrossRef](#)]



© 2018 by the authors. Licensee MDPI, Basel, Switzerland. This article is an open access article distributed under the terms and conditions of the Creative Commons Attribution (CC BY) license (<http://creativecommons.org/licenses/by/4.0/>).